IEEE Access
Multidisciplinary : Rapid Review : Open Access Journal

Received 29 March 2023, accepted 18 April 2023, date of publication 12 May 2023, date of current version 18 May 2023.

Digital Object Identifier 10.1109/ACCESS.2023.3275755

RESEARCH ARTICLE

RIS-Assisted Multi-User MIMO Systems Exploiting Extreme Learning Machine

M. REZWANUL MAHMOOD[1], MOHAMMAD ABDUL MATIN[1], (Senior Member, IEEE), AND SOTIRIOS K. GOUDOS[2], (Senior Member, IEEE)

[1]Department of Electrical and Computer Engineering, North South University, Dhaka 1229, Bangladesh
[2]ELEDIA@AUTH, Department of Physics, Aristotle University of Thessaloniki, 54124 Thessaloniki, Greece

Corresponding author: Mohammad Abdul Matin (mohammad.matin@northsouth.edu)

ABSTRACT Massive multiple-input multiple-output (mMIMO), assisted by reconfigurable intelligent surface (RIS), can ensure reliable and energy-efficient data transmission. However, the receiver design for large-scale networks based on traditional mathematical approaches requires complex statistics. Therefore, in this paper, machine learning (ML) approaches are investigated to design receivers for the RIS-assisted multi-user MIMO (muMIMO) systems to avoid complicated channel information requirements. Extreme learning machine (ELM) is an effective ML tool for MIMO receiver design because it simplifies the learning process. However, the learning performance of the ELM can get affected by the random choice of its hidden layer size. To address this issues, this paper proposes an incremental ELM (I-ELM) based receiver for the RIS-mu-MIMO system. The proposed receiver computes the weights between the hidden and the output layer based on the automated incremental addition of hidden neurons and provided conditions. The suggested receiver is contrasted with the multilayer perceptron (MLP), conventional ELM, and minimum mean square error (MMSE) receivers. The simulation results show that the throughput performance of the proposed receiver is satisfactory.

INDEX TERMS Extreme learning machine, intelligent surface, machine learning, massive MIMO, multi-layer perceptron.

I. INTRODUCTION

Massive multiple-input multiple-output (mMIMO) is acknowledged as a key enabler for future wireless network systems [1], [2]. The deployment of large number of antennas in mMIMO provides improved spectral efficiency and massive IoT device connectivity with high throughput. These large antenna arrays can assist in producing directional beams that can reduce propagation loss at high frequency spectrum, but the directed beams suffer from blockage. To overcome this phenomenon, additional relays and base stations (BSs) can be implemented, which in turn increase the implementation cost and power consumption.

In recent times, reconfigurable intelligent surface (RIS) has attracted a lot of attention due to its capability in changing EM wave properties, such as amplitude and phase [3]. This provides the opportunity to improve the energy of received signal as well as coverage area, and prevent signal leakage to the undesired user. Compared to conventional relays, such as amplify-and forward (AF), decode-and-forward (DF), RIS consumes less amount of power to amplify the signal without introducing any noise ideally [4]. Thus, RIS assisted MIMO system provides cost and energy efficient 6G network systems. Our research is focused on to design a receiver for RIS-multi-user MIMO (RIS-muMIMO) system.

A. RELATED WORKS

In general, channel estimation (CE) is required to design a MIMO receiver [5]. In an RIS-muMIMO system, CE becomes more crucial since its mathematical modeling involves amplitude attenuation and phase shifts [3]. As a result, much research efforts have been provided to estimate RIS-MIMO channels that would aid in designing a receiver. A two stage channel estimation approach is presented in [6],

The associate editor coordinating the review of this manuscript and approving it for publication was Vladimir Poulkov.

where first stage of the proposed CSI estimation approach uses the traditional uplink training method to determine the direct MIMO channel between the access point (AP) and the users and the second stage of the proposed approach estimates the AP-RIS channel and the RIS-user channel. In [7], the CE involves estimation of the direction-of-arrival (DoA) and path gains. Channel parameters such as angle of departures (AoDs) of BS-RIS channels, angle of arrivals (AoAs) of the RIS-user end channels, angle differences and product of the path gains in a RIS-mmWave-MIMO system are estimated in [8]. In [9], the CE problem is formulated as DoA estimation problem. In [10], maximum achievable rate of the RIS-MIMO system is attempted to obtain by means of the proposed CE and the passive beamforming [11] schemes. The reflection coefficients of the RIS are considered to be pre-designed and the effective superposed channel is estimated. The beamformer is designed on the basis of the estimated superposed channel. In [12], minimum mean square error (MMSE)-based approaches are studied for CE and the design of phase shifts and equalizer. Estimation of the composite channel, which is the direct channel between the user and BS and cascaded channel among the user, RIS and BS, is also analyzed in the study.

With the increase of the number of users, complexities in network performance analysis will also increase. Difficulties in ensuring QoS demands of the users will also rise. Machine learning (ML)-based methods is seen as a potential tool for the future network systems, including RIS-based networks [13]. A deep learning (DL) framework, presented in [14], consists of a twin convolutional neural network (CNN) architecture that estimates both the direct link and cascaded link channels by analyzing the received pilot signals. The research work conducted in [15] uses a three-stage training approach with deep neural network (DNN) to estimate the CSI of direct communication link as well as the cascaded CSI for both the active and inactive RIS components. A deep residual learning-based CSI estimation approach is presented in [16]. A convolutional neural network architecture is used that utilizes the spatial properties of the noisy channel matrices as well as the cumulative behavior of the noise. In [17], the training of a deep neural network with the aid of unsupervised learning technique is performed for designing passive beamforming [11] matrices in an RIS-enabled network system. The joint design of the transmit beamformer and phase shift matrix is performed by means of deep reinforcement learning (DRL) algorithm in [18]. The transmit beamforming and phase shift matrices are both said to be obtained concurrently by the proposed approach at the neural network's output. However, DL-based approaches require complicated parameter adjustment through backpropagation algorithm, which can be expensive in terms of duration. In such case, extreme learning machine (ELM) can be implemented.

An ELM-based receiver is designed in [19] for a light-emitting diode (LED)-based MIMO system. The ELM receiver is constructed on real domain base. ELM-based approach can also be extended to complex domain applications, which are observed in [20], [21], and [22]. In [20], the ELM is trained offline first with the training data and then deployed online. However, the ELM algorithm can be both trained and deployed online, which is demonstrated in [21]. Least square (LS)-based channel estimation is conducted first and the symbols are equalized, based on the estimated channel. Then the online trained ELM is used to refine the equalization process [22]. Therefore, in this paper, the online ELM algorithm is explored for designing RIS-MIMO receiver. The traditional ELM, implemented in the above studies, is not immune to the random choice of the hidden layer size. It will not provide satisfactory performance if the hidden layer size is too small or large. Therefore, to address this issue, an incremental constructive approach for the ELM algorithm-based method is presented.

B. CONTRIBUTION OF THE PAPER

In an incremental ELM (I-ELM) algorithm, the hidden neurons are randomly chosen. Based on given specifications, it is able to adjust the hidden layer size and provide descent prediction performance. Therefore, an I-ELM algorithm is proposed in this paper to design a receiver for an RIS-muMIMO system. The main contributions of the paper is summarized as follows.

- An I-ELM receiver is proposed for an RIS-assisted muMIMO systems with a single BS, a single RIS unit and several users.
- The proposed receiver is compared to the MMSE, the traditional ELM and the multilayer perceptron (MLP) receivers in terms of throughput performance for a given RIS-muMIMO system configuration. Furthermore, comparative studies are also conducted for different BS antennas and RIS elements. It is shown that the proposed I-ELM provide satisfactory performance with respect to the other receivers.

The paper is organized as follows. The RIS-muMIMO system model and receiver design with traditional mathematical approach in section II. ELM based receiver is discussed in section III. Architecture of I-ELM is described in section IV. Simulation results are provided in V. The paper is concluded with section VI.

II. SYSTEM MODEL OF RIS-muMIMO

In this paper, an uplink communication system is considered, as shown in Fig. 1, where the single BS contains N_R antennas, the RIS unit contains M elements and K users contain N_T antennas. The user-base station direct link, the user-RIS link and the RIS-base station link are denoted by $\boldsymbol{H}_{d,k} \in \mathbb{C}^{N_R \times N_T}$, $\boldsymbol{F}_k \in \mathbb{C}^{M \times N_T}$ and $\boldsymbol{G} \in \mathbb{C}^{N_R \times M}$ respectively. These channel matrices follow Rayleigh distribution. A total of N subcarrier frequencies are used for transmitting data symbols, where $N_k = \frac{N}{K}$ orthogonal subcarriers are allocated to each users. Cyclic prefix-orthogonal frequency division multiplexing (CP-OFDM) protocol with 120 kHz of subcarrier spacing is followed by the system. The channel coded bits are digitally modulated, based on the normalized

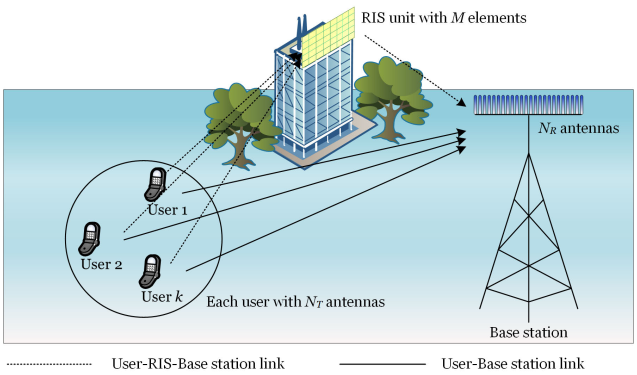

FIGURE 1. System model of RIS-assisted mu-MIMO system.

modulation power. The inverse discrete Fourier transform operation (IDFT) is executed on these normalized modulated data and transmitted through the direct and cascaded channel links. The received time domain signal at the base station is

$$\boldsymbol{y} = \sum_{k=1}^{K} (\boldsymbol{H}_{d,k} + \boldsymbol{G\Phi F}_k)\boldsymbol{x}_k + \boldsymbol{z} \tag{1}$$

Here, the transmitted signal by the user k is represented by $\boldsymbol{x}_k$. The noise is denoted by $\boldsymbol{z}$ with the characteristics $\mathcal{CN}(0, \sigma^2)$, where σ^2 is the noise power. The amplitude attenuation α_i and the phase shifts ϕ_i, occurred at each RIS element ($i = 1, 2, \ldots, M$), are respectively represented by the following diagonal matrix.

$$\boldsymbol{\Phi} = diag[\alpha_1 e^{j\phi_1}, \alpha_2 e^{j\phi_2}, \ldots, \alpha_M e^{j\phi_M}], \tag{2}$$

where $\alpha_i \in [0, 1]$ and $\phi_i \in [0, 2\pi)$. No signal attenuation on the RIS is considered, thus $\alpha_i = 1$ is considered in this paper [23]. Furthermore, the phase shifts are derived according to [6].

At the receiving end, the CP is removed from the received signal and discrete Fourier transform operation (DFT) is executed. The received symbol $\boldsymbol{Y}_k \in \mathbb{C}^{N_R \times N_{UT}}$ at the base station corresponding to the UT k is given by

$$\begin{aligned}\boldsymbol{Y}_k &= DFT(\boldsymbol{H}_{d,k} + \boldsymbol{G\Phi F}_k)\boldsymbol{X}_k \\ &\quad + \sum_{i=1, i\neq k}^{K} DFT(\boldsymbol{H}_{d,i} + \boldsymbol{G\Phi F}_i)\boldsymbol{X}_i + DFT(\boldsymbol{Z}) \end{aligned} \tag{3}$$

The above equation is further simplified as follows.

$$\boldsymbol{Y}_k = \boldsymbol{H}_k\boldsymbol{X}_k + \sum_{i=1, i\neq k}^{K} \boldsymbol{H}_i\boldsymbol{X}_i + \boldsymbol{Z}. \tag{4}$$

Here, $\boldsymbol{H}_k = DFT(\boldsymbol{H}_{d,k} + \boldsymbol{G\Phi F}_k)$, $\boldsymbol{H}_i = DFT(\boldsymbol{H}_{d,i} + \boldsymbol{G\Phi F}_i)$, $\boldsymbol{X}_k = DFT(\boldsymbol{x}_k)$ and $\boldsymbol{X}_i = DFT(\boldsymbol{x}_i)$. In this paper, the composite channel, $\hat{\boldsymbol{H}}_k$, is aimed to be estimated for the user k by using the reference symbols (transmitted with the data symbols), which is known at the receiving end (i.e. base station).

A. RECEIVER DESIGN BY MEANS OF CHANNEL INFORMATION

With the help of the estimated channel information, traditional linear receiver(s) equalizes the received symbols. If the transmitted reference symbols are $\boldsymbol{X}_{\rho,k}$ and the received reference symbols are $\boldsymbol{Y}_{\rho,k}$, then the CE by means of LS estimation technique [24] is

$$\hat{\boldsymbol{H}}_{k,LS} = \boldsymbol{Y}_{\rho,k}\boldsymbol{X}_{\rho,k}^{-1}. \tag{5}$$

To minimize the mean square error (MSE) of the LS channel estimation, a Bayesian-based MMSE estimation method can be used [25], [26], which gives the following equation.

$$\hat{\boldsymbol{H}}_k = \sigma^2_{\hat{\boldsymbol{H}}_{k,LS}}(\sigma^2_{\hat{\boldsymbol{H}}_{k,LS}} + \sigma_k^2)^{-1}\hat{\boldsymbol{H}}_{k,LS}. \tag{6}$$

Here, the estimated channel variance is denoted by $\sigma^2_{\hat{\boldsymbol{H}}_{k,LS}}$. With the help of MMSE-based CE, that is, $\hat{\boldsymbol{H}}_k$, channel equalization is performed on the received data.

$$\hat{\boldsymbol{X}}_{k,MMSE} = (\hat{\boldsymbol{H}}_k^*\hat{\boldsymbol{H}}_k + \sigma_k^2\boldsymbol{I})^{-1}\hat{\boldsymbol{H}}_k^*\boldsymbol{Y}_k = \boldsymbol{V}_k\boldsymbol{Y}_k. \tag{7}$$

To extract the transmitted bits, digital demodulation on the equalized symbols and channel decoding operations are performed.

B. THROUGHPUT DETERMINATION

The throughput of the user k is determined from the following expression.

$$R_k = B\log_2(1 + SINR_k). \tag{8}$$

Here, the allocated bandwidth for each user is denoted by B. The signal-to-noise ratio is represented by $SINR_k$, which is generally defined as follows.

$$SINR_k = \frac{|\boldsymbol{V}_k^*\hat{\boldsymbol{H}}_k|^2}{(\sum_{i=1,i\neq k}^{K}|\boldsymbol{V}_k^*\hat{\boldsymbol{H}}_i|^2 + \sum_{i=1}^{K}\boldsymbol{V}_k^*\boldsymbol{C}_k\boldsymbol{V}_k + ||\boldsymbol{V}_k||^2)} \tag{9}$$

Here, the corresponding estimation error covariance matrix is denoted by $\boldsymbol{C}_k$. However, the ELM algorithm does not explicitly determine channel information. Therefore, $SINR_k$ is determined by adopting the following equation.

$$SINR_k = -[PAPR + 20\log_{10}(EVM_k/100\%)]. \tag{10}$$

Here, $PAPR$ represents peak-to-average-power ratio and EVM_k represents the error vector magnitude. Peak-to-average-power ratio value is chosen according to the digital modulation strategy. The error vector magnitude is determined by calculating the Euclidean distance between the originally transmitted and received modulated symbols.

III. PRELIMINARY KNOWLEDGE OF THE ELM ALGORITHM

In this section, a three-layered traditional extreme learning architecture is described, as shown in Fig. 2. The input layer, hidden layer and output layer contains N_R, L and N_T neurons respectively. The ELM is assigned with random input weights

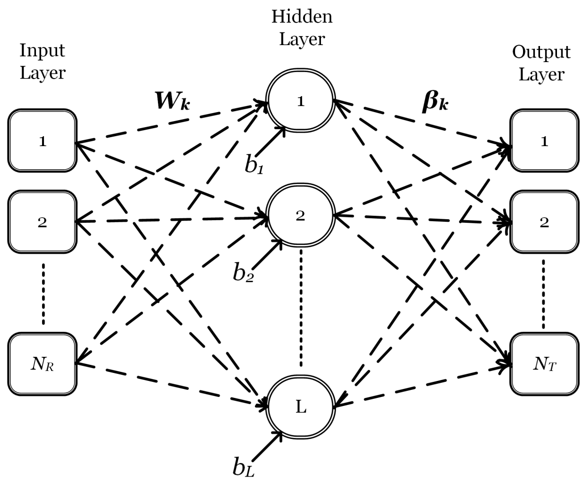

FIGURE 2. **Architecture of traditional extreme learning machine.**

$W_k \in \mathbb{C}^{L\times N_R}$ and biases $b_k \in \mathbb{C}^{L\times 1}$. The input layer is fed with the received signals received at each antenna. On the basis of a chosen activation function, the hidden layer output is computed from the input data. The desired output is obtained at the output layer after the ELM network is trained. Different from the backpropagation approach based ML networks to update the weights W_k and biases b_k ($b_k = b_1, b_2, \ldots, b_L$), the ELM uses an output weight $\beta_k \in \mathbb{C}^{L\times N_T}$ (between the hidden layer and the output layer). It is calculated in training phase from the hidden layer output and the desired output (from the training data).

The transmitted and received reference symbols are considered as training datasets, expressed as

$$T_k = (Y_{\rho,k}, X_{\rho,k}),$$

for the ELM training. The hidden layer output $D_{\rho,k}$ for the received reference symbols is calculated from $Y_{\rho,k}$ (received reference symbols), W_k and b_k as follows.

$$D_{\rho,k} = a((W_k Y_{\rho,k} + b_k)^T). \tag{11}$$

Here, $a(.)$ is the activation function. The output weights β_k can be determined from $D_{\rho,k}$ and transmitted reference symbols $X_{\rho,k}$, by finding the least square solution of the problem $D_{\rho,k}\beta_k = X^T_{\rho,k}$.

$$\beta_k = (D^{\dagger}_{\rho,k} D_{\rho,k})^{-1} D^{\dagger}_{\rho,k} X^T_{\rho,k}. \tag{12}$$

The received data symbols Y_k is then provided into the input layer of the trained ELM receiver. The hidden layer output D_k for the received data symbols is then computed as follows.

$$D_k = a(W_k Y_k + b_k). \tag{13}$$

By using the computed output weight β_k, the transmitted symbols is determined from D_k.

$$X_{ELM,k} = \beta^T_k D_k. \tag{14}$$

Algorithm 1 Summary of ELM-Based Receiver Design Mechanism

Training pilot symbol sets $T_k = Y_{\rho,k}, X_{\rho,k}$ for user k, hidden layer with L number of neurons and activation function $a(.)$

TRAINING PHASE
- Random generation of W_k and b_k.
- Determination of $D_{\rho,k}$ from (11).
- Determination of β_k from (12).

TESTING PHASE
- Determination of D_k from (13).
- Estimation of $X_{ELM,k}$ from (14).

The equalized symbols by means of ELM algorithm is denoted by $X_{ELM,k} \in \mathbb{C}^{N_T\times N_k}$. The ELM algorithm is summarized in 1.

IV. PROPOSED RECEIVER FOR THE RIS-muMIMO SYSTEM

In this section, the working mechanism of the I-ELM is discussed with a view to designing RIS-muMIMO receiver. Fig. 3 represents the training architecture of the I-ELM receiver. Let us assume that the ELM network has L_i initially assigned neurons. The initial input weights and biases would be $W_{k,i} \in \mathbb{C}^{L_i\times N_R}$ and $b_{k,i} \in \mathbb{C}^{L_i\times 1}$ respectively. The hidden layer output for received reference symbols would be expressed as follows.

$$D_{\rho,k,i} = a((W_{k,i} Y_{\rho,k} + b_{k,i})^T). \tag{15}$$

The output weight for L_i hidden layer neurons would be

$$\beta_{k,i} = (D^{\dagger}_{\rho,k,i} D_{\rho,k,i})^{-1} D^{\dagger}_{\rho,k,i} X^T_{\rho,k}. \tag{16}$$

The equations (13) and (14) would be used to estimate the transmitted reference symbols for L_i hidden neurons.

$$D_{k,i} = a(W_{k,i} Y_{\rho,k} + b_{k,i}). \tag{17}$$

$$X_{I-ELM,\rho,k,i} = \beta^T_{k,i} D_{k,i}. \tag{18}$$

If the number of hidden neurons is not appropriately chosen, then an error (say, MSE $= \xi_\rho$) will exist between $X_{\rho,k}$ and $X_{I-ELM,\rho,k,i}$. The I-ELM network will then keep adding hidden layer neurons until ξ_ρ is minimized to an expected value $\xi_{\rho,exp}$. A maximum allowable number of hidden layer neurons, L_{max} is also assigned to control the addition of hidden neurons.

After the training of I-ELM, input weights $W_{k,new}$, biases $b_{k,new}$ and output weights $\beta_{k,new}$ for the hidden layer with L_{new} neurons. The testing of I-ELM is similar to the traditional ELM. The I-ELM receiver mechanism is summarized in 2.

With the increase of hidden layer neurons, the prediction accuracy improves. However, too many hidden layer neurons may increase the load on the computational resources. In this case, I-ELM algorithm is advantageous for automatically

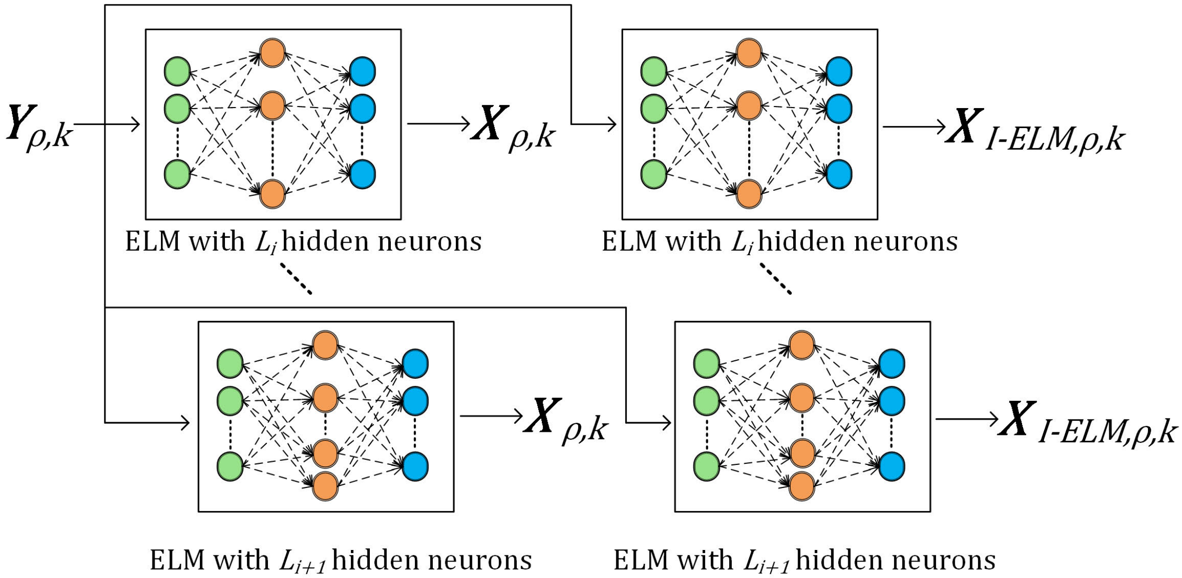

FIGURE 3. **Block diagram of the training phase of I-ELM receiver. This phase of the proposed receiver continues until ξ_ρ and L_i criteria are met.**

handling of the hidden layer size and consequently deliver satisfactory prediction performance.

V. SIMULATION RESULTS AND DISCUSSIONS

In this section, the simulation results obtained for the RIS-muMIMO system with center frequency of 30 GHz is presented. The spacing among the subcarrier frequencies is 120 kHz. Four users ($K = 4$, with $N_T = 2$ transmitting antenna each), single BS with $N_R = 64$ and single RIS unit with $M = 64$ are initially considered for the study. The number of total subcarrier is $N = 960$, which is divided equally among the 4 users. In other words, the number of allocated subcarrier for each user is $N_k = 240$. Low-density parity check (LDPC) with 1/2 code rate is applied to the data bits. The modulation format is elected to be 16-quadrature amplitude modulation (16-QAM). The signal-to-noise ratio is defined as $\frac{\mathbb{E}[|\mathbf{x}_k|^2]}{\sigma^2}$. The ELM algorithms (both traditional and proposed) are trained with the transmitted and received symbols (corresponding to the user k) at one OFDM symbol time, out of 14 OFDM symbol times. Activation function *tanh* is chosen for the hidden layer of both of the ELM receivers. The input weights and the biases are assigned by random complex numbers within $[-10^{-2}, 10^{-2}]$. This interval is chosen such that the weight and the bias values fall within the activation function's region of convergence [22]. Based on the study conducted in [27], the number of hidden layer neurons in the traditional ELM is considered to be $L = max(N_R, N_T)$. In case of I-ELM receiver, the initial hidden layer size L_i and the maximum number of hidden layer neurons, i.e. L_{max}, are considered to be equal to 10 and $max(N_R, N_T)$ respectively. The expected minimum MSE value $\xi_{\rho,exp}$ for I-ELM receiver is chosen to be 0.01.

Algorithm 2 I-ELM-Based Receiver Mechanism

Training pilot symbol sets $\boldsymbol{T}_k = \boldsymbol{Y}_{\rho,k}, \boldsymbol{X}_{\rho,k}$ for user k, activation function $a(.)$, initial hidden layer neurons L_i, maximum hidden layer neurons L_{max} and $\xi_\rho = \xi_{\rho,exp}$.

TRAINING PHASE

- Initialization of $\boldsymbol{W}_{k,i}$ and $\boldsymbol{b}_{k,i}$ for given L_i.
- Computation of $\boldsymbol{\beta}_{k,i}$ from (15) and (16).
- Estimation of $\boldsymbol{X}_{I-ELM,\rho,k,i}$ from (17) and (18).
- Determination of ξ between $\boldsymbol{X}_{\rho,k}$ and $\boldsymbol{X}_{I-ELM,\rho,k,i}$.
- While $L_i \leq L_{max}$ and $\xi_\rho \geq \xi_{\rho,exp}$
  - L_i is expanded to L_{i+1} for adding single hidden layer neuron each time.
  - Expansion of $\boldsymbol{W}_{k,i}$ and $\boldsymbol{b}_{k,i}$ to $\boldsymbol{W}_{k,i+1}$ and $\boldsymbol{b}_{k,i+1}$ for the newly added hidden layer neuron.
  - Computation of $\boldsymbol{\beta}_{k,i+1}$ by following (15) and (16).
  - Estimation of $\boldsymbol{X}_{I-ELM,\rho,k,i+1}$ for the newly determined $\boldsymbol{\beta}_{k,i+1}$ according to (17) and (18) and computation of ξ_ρ between $\boldsymbol{X}_{\rho,k}$ and $\boldsymbol{X}_{I-ELM,\rho,k,i+1}$.

TESTING PHASE

- Given, L_{new}, $\boldsymbol{W}_{k,new} \in \mathbb{C}^{L_{new}\times N_R}$, $\boldsymbol{b}_{k,new} \in \mathbb{C}^{L_{new}\times 1}$ and $\boldsymbol{\beta}_{k,new}$.
  - $\boldsymbol{D}_{k,new} = a(\boldsymbol{W}_{k,new}\boldsymbol{Y}_k + \boldsymbol{b}_{k,new})$.
  - $\boldsymbol{X}_{I-ELM,k,new} = \boldsymbol{\beta}^T_{k,new}\boldsymbol{D}_{k,new}$.

A. ANALYSIS OF THROUGHPUT PERFORMANCES

The performance of the proposed I-ELM receiver is compared to that of the MMSE, traditional ELM and MLP

TABLE 1. Simulation parameters.

Parameter	Value	Parameter	Value
N_R	16, 32, 64, 128	N_T	2
M	64, 100, 144, 196, 256	N	960
K	4	N_k	240
Center frequency	30 GHz	SNR (dB)	0–30

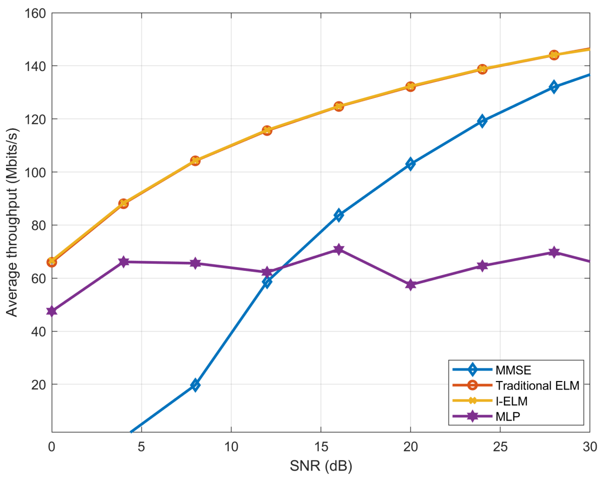

FIGURE 4. Average throughput obtained by means of the MMSE, traditional ELM, I-ELM and MLP receiver.

receiver. An MLP algorithm [28], which is a DNN-based algorithm, is used to design a receiver for comparing its performance with the ELM-based receivers. According to [25], the MLP algorithm uses each neuron for real and imaginary part of the complex numbers respectively. Therefore, the MLP-based receiver is constructed such that the real and the imaginary part of the received symbols are separated for training and equalization. The input layer of the MLP contains 2 N_R neurons and the output layer contains 2 N_T neurons. The MLP receiver has 4 hidden layers. The number of neurons in the successive hidden layers are 64, 32, 16 and 8. The activation function chosen for each of the hidden layers is *tanh*. To update the weight parameters, the learning rate of 0.005 and momentum of 0.9 are assigned. In Fig. 4, both of the ELM receivers have shown better throughput performance with respect to the MMSE and the MLP receiver for the RIS-muMIMO system with 2 transmitting antennas and 64 receiving antennas. The MMSE receiver achieves low throughput performance at lower SNR values due to imperfect channel estimation. At SNR $=$ 30 dB, about 6 Mbits/s more is achieved by the ELM receivers than the MMSE receiver. For SNR values between $0 - 28$ dB, both the ELM receivers utilize $L = 64$ neurons in the hidden layers for all user data. However, for the SNR value above 28 dB, the lowest and highest values of L are 39 and 64 respectively for the I-ELM receiver, whereas, the traditional ELM utilizes $L = 64$ neurons. This demonstrates that the I-ELM receiver has enough throughput performance that is comparable to the traditional ELM receiver while also reducing computational complexities. It can adapt the hidden layer size as necessary based on the provided criteria, such as L_{max} and $\xi_{\rho,exp}$.

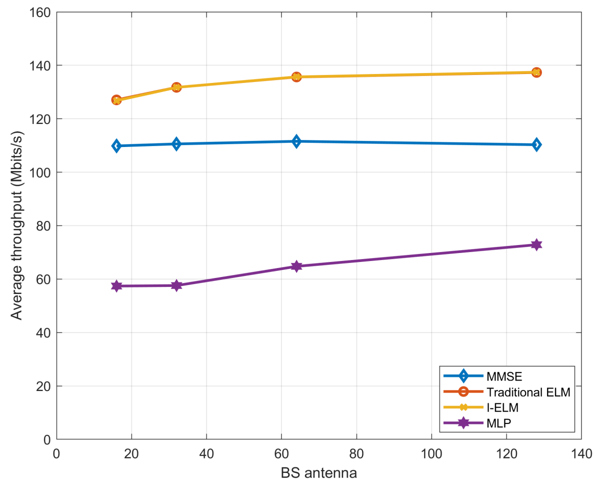

FIGURE 5. Average throughput as a function of BS antennas by means of MMSE, traditional ELM, I-ELM and MLP receivers.

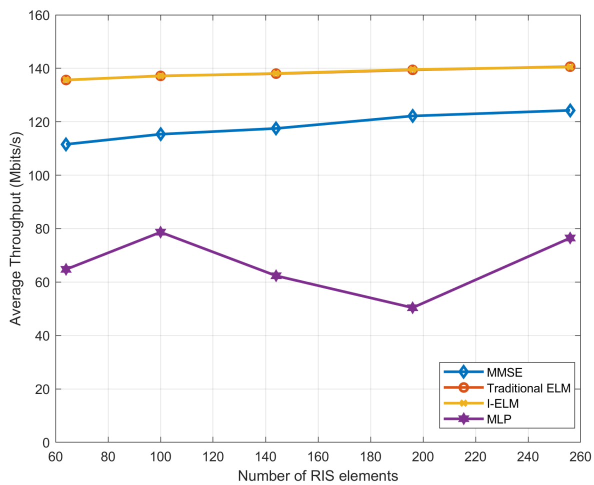

FIGURE 6. Average throughput as a function of RIS elements by means of MMSE, traditional ELM, I-ELM and MLP receivers.

B. EVALUATION OF THE RECEIVERS FOR RIS-muMIMO CONFIGURATION

In this section, the presented RIS-muMIMO receivers are evaluated by varying the BS antennas and the RIS elements respectively, which can increase the throughput of the RIS-muMIMO systems [3], [29]. Here, the expected MSE, ξ_ρ is kept 0.01. In Fig. 5, the MMSE, traditional ELM, I-ELM and MLP receivers are evaluated in terms of throughput performance for 64 RIS elements and different BS antennas (as mentioned in Table 1) at SNR $=$ 22. As the BS antennas are increased from 16 to 32, noticeable improvement is observed for both of the ELM receivers. However, by increasing BS antennas from 32 to 128, the throughput performance is increased by small margin. On the other hand, the throughput performance marginally increases by means of MMSE receiver. In Fig. 6, the MMSE, traditional ELM, I-ELM and MLP receivers are evaluated for the RIS-muMIMO system with 64 receiving antennas and different RIS elements, as mentioned in Table 1, at SNR $= 22$. With the increase of RIS elements, the throughput performance achieved by employing the MMSE and both the ELM receivers improved. The ELM receivers prevail its superiority over the MMSE and the MLP receiver. The complexity of the receivers are discussed in the following subsection.

1) COMPLEXITY OF THE RECEIVERS

Following the expression, $KN_k(3N_T^2N_R + 2N_R^2N_T - N_R^2 + \frac{2}{3}N_T^3 + N_TN_R)$, the MMSE receiver requires a total of 12661760 mathematical operations for symbol detection, whereas, $2KN_k(L_a2N_R+L_aL_b+L_bL_c+L_cL_d+L_d2N_T)$ mathematical operations are required for trained MLP receiver. Here, $L_a = 64$, $L_b = 32$, $L_c = 16$ and $L_d = 8$. Therefore, a total of 20951040 mathematical operations are required for MLP receiver. The expression for complexity of the trained ELM receivers is $KN_k(2LN_R + L + 2LN_T - N_T)$. The traditional ELM receiver performs 8169600 mathematical operations at all SNR values, whereas, at SNR values above 28 dB (Fig. 4), the I-ELM receiver performs less number of operations with 39 neurons (lowest value of L), which is 4977600. This demonstrates that the I-ELM receiver has comparable throughput to the traditional ELM receiver while also reducing computational complexities.

VI. CONCLUSION

In this paper, an I-ELM-based receiver is proposed for the RIS-muMIMO system. Based on the provided specifications, this ML architecture adjusts the hidden layer size and minimizes the overall performance error. For a given RIS-muMIMO system, the I-ELM receiver is compared to the MMSE, traditional ELM and MLP receivers in terms of throughput. Performance evaluation is done for different BS antennas and RIS elements. In all cases, the I-ELM receiver performs better than MMSE and MLP receivers.

REFERENCES

[1] S. Khwandah, J. Cosmas, P. Lazaridis, Z. Zaharis, and I. Chochliouros, "Massive MIMO systems for 5G communications," *Wireless Pers. Commun.*, vol. 120, no. 3, pp. 2101–2115, 2021.

[2] C. Xu, J. Cosmas, Y. Zhang, P. Lazaridis, G. Araniti, and Z. D. Zaharis, "3D MIMO radio channel modeling of a weighted linear array system of antennas for 5G cellular systems," in *Proc. Int. Conf. Telecommun. Multimedia (TEMU)*, Jul. 2016, pp. 1–6.

[3] P. Mursia, V. Sciancalepore, A. Garcia-Saavedra, L. Cottatellucci, X. C. Pérez, and D. Gesbert, "RISMA: Reconfigurable intelligent surfaces enabling beamforming for IoT massive access," *IEEE J. Sel. Areas Commun.*, vol. 39, no. 4, pp. 1072–1085, Apr. 2021.

[4] H. Zhang, S. Ma, Z. Shi, X. Zhao, and G. Yang, "Sum-rate maximization of RIS-aided multi-user MIMO systems with statistical CSI," *IEEE Trans. Wireless Commun.*, early access, Dec. 19, 2022, doi: 10.1109/TWC.2022.3228910.

[5] S. Zettas, S. Kasampalis, P. Lazaridis, Z. D. Zaharis, and J. Cosmas, "Channel estimation for OFDM systems based on a time domain pilot averaging scheme," in *Proc. 16th Int. Symp. Wireless Pers. Multimedia Commun. (WPMC)*, 2013, pp. 1–6.

[6] J. Mirza and B. Ali, "Channel estimation method and phase shift design for reconfigurable intelligent surface assisted MIMO networks," *IEEE Trans. Cognit. Commun. Netw.*, vol. 7, no. 2, pp. 441–451, Jun. 2021.

[7] X. Chen, J. Shi, Z. Yang, and L. Wu, "Low-complexity channel estimation for intelligent reflecting surface-enhanced massive MIMO," *IEEE Wireless Commun. Lett.*, vol. 10, no. 5, pp. 996–1000, May 2021.

[8] J. He, H. Wymeersch, and M. Juntti, "Channel estimation for RIS-aided mmWave MIMO systems via atomic norm minimization," *IEEE Trans. Wireless Commun.*, vol. 20, no. 9, pp. 5786–5797, Sep. 2021.

[9] K. Ardah, S. Gherekhloo, A. L. F. de Almeida, and M. Haardt, "TRICE: A channel estimation framework for RIS-aided millimeter-wave MIMO systems," *IEEE Signal Process. Lett.*, vol. 28, pp. 513–517, 2021.

[10] J. An, C. Xu, L. Gan, and L. Hanzo, "Low-complexity channel estimation and passive beamforming for RIS-assisted MIMO systems relying on discrete phase shifts," *IEEE Trans. Commun.*, vol. 70, no. 2, pp. 1245–1260, Feb. 2022.

[11] W. Yan, X. Yuan, and X. Kuai, "Passive beamforming and information transfer via large intelligent surface," *IEEE Wireless Commun. Lett.*, vol. 9, no. 4, pp. 533–537, Apr. 2020.

[12] O. T. Demir and E. Bjornson, "Is channel estimation necessary to select phase-shifts for RIS-assisted massive MIMO?" *IEEE Trans. Wireless Commun.*, vol. 21, no. 11, pp. 9537–9552, Nov. 2022.

[13] M. R. Mahmood, M. A. Matin, P. Sarigiannidis, and S. K. Goudos, "A comprehensive review on artificial intelligence/machine learning algorithms for empowering the future IoT toward 6G era," *IEEE Access*, vol. 10, pp. 87535–87562, 2022.

[14] A. M. Elbir, A. Papazafeiropoulos, P. Kourtessis, and S. Chatzinotas, "Deep channel learning for large intelligent surfaces aided mm-wave massive MIMO systems," *IEEE Wireless Commun. Lett.*, vol. 9, no. 9, pp. 1447–1451, Sep. 2020.

[15] S. Gao, P. Dong, Z. Pan, and G. Y. Li, "Deep multi-stage CSI acquisition for reconfigurable intelligent surface aided MIMO systems," *IEEE Commun. Lett.*, vol. 25, no. 6, pp. 2024–2028, Jun. 2021.

[16] C. Liu, X. Liu, D. W. K. Ng, and J. Yuan, "Deep residual learning for channel estimation in intelligent reflecting surface-assisted multi-user communications," *IEEE Trans. Wireless Commun.*, vol. 21, no. 2, pp. 898–912, Feb. 2022.

[17] J. Gao, C. Zhong, X. Chen, H. Lin, and Z. Zhang, "Unsupervised learning for passive beamforming," *IEEE Commun. Lett.*, vol. 24, no. 5, pp. 1052–1056, May 2020.

[18] C. Huang, R. Mo, and C. Yuen, "Reconfigurable intelligent surface assisted multiuser MISO systems exploiting deep reinforcement learning," *IEEE J. Sel. Areas Commun.*, vol. 38, no. 8, pp. 1839–1850, Aug. 2020.

[19] D. Gao and Q. Guo, "Extreme learning machine-based receiver for MIMO LED communications," *Digit. Signal Process.*, vol. 95, Dec. 2019, Art. no. 102594.

[20] C. Qing, L. Wang, L. Dong, and J. Wang, "Enhanced ELM based channel estimation for RIS-assisted OFDM systems with insufficient CP and imperfect hardware," *IEEE Commun. Lett.*, vol. 26, no. 1, pp. 153–157, Jan. 2022.

[21] J. Liu, K. Mei, X. Zhang, D. Ma, and J. Wei, "Online extreme learning machine-based channel estimation and equalization for OFDM systems," *IEEE Commun. Lett.*, vol. 23, no. 7, pp. 1276–1279, Jul. 2019.

[22] D. F. Carrera, D. Zabala-Blanco, C. Vargas-Rosales, and C. A. Azurdia-Meza, "Extreme learning machine-based receiver for multi-user massive MIMO systems," *IEEE Commun. Lett.*, vol. 25, no. 2, pp. 484–488, Feb. 2021.

[23] B. Sheen, J. Yang, X. Feng, and M. M. U. Chowdhury, "A deep learning based modeling of reconfigurable intelligent surface assisted wireless communications for phase shift configuration," *IEEE Open J. Commun. Soc.*, vol. 2, pp. 262–272, 2021.

[24] Y. S. Cho, J. Kim, W. Y. Yang, and C. G. Kang, *MIMO-OFDM Wireless Communications With MATLAB*. Singapore: Wiley, 2010.

[25] D. F. Carrera, C. Vargas-Rosales, N. M. Yungaicela-Naula, and L. Azpilicueta, "Comparative study of artificial neural network based channel equalization methods for mmWave communications," *IEEE Access*, vol. 9, pp. 41678–41687, 2021.

[26] D. F. Carrera, C. Vargas-Rosales, L. Azpilicueta, and J. A. Galaviz-Aguilar, "Comparative study of channel estimators for massive MIMO 5G NR systems," *IET Commun.*, vol. 14, no. 7, pp. 1175–1184, Apr. 2020.

[27] M. R. Mahmood, M. A. Matin, P. Sarigiannidis, S. K. Goudos, and G. K. Karagiannidis, "Residual compensation-based extreme learning machine for MIMO-NOMA receiver," *IEEE Access*, vol. 11, pp. 13398–13407, 2023.
[28] L. Noriega, "Multilayer perceptron tutorial," School Comput., Staffordshire Univ., Staffordshire, U.K., Tech. Rep., 2005.
[29] P. Wang, J. Fang, L. Dai, and H. Li, "Joint transceiver and large intelligent surface design for massive MIMO mmWave systems," *IEEE Trans. Wireless Commun.*, vol. 20, no. 2, pp. 1052–1064, Feb. 2021.

M. REZWANUL MAHMOOD received the B.S. degree in electrical and electronic engineering from East West University, Dhaka, Bangladesh, in 2017. He is currently pursuing the M.S. degree in electrical and electronic engineering with North South University, Dhaka. He is a Research Assistant with North South University. He has published few papers in reputed journals and international conferences. His research interests include future wireless networks, the Internet of Things, and machine learning.

MOHAMMAD ABDUL MATIN (Senior Member, IEEE) received the B.Sc. degree in electrical and electronic engineering from BUET, Bangladesh, the M.Sc. degree in digital communication from Loughborough University, U.K., and the Ph.D. degree in wireless communication from Newcastle University, U.K. He has been a Professor with the Department of Electrical and Computer Engineering, North South University (NSU), since 2008. He has published over 120 peer-reviewed journals and conference papers. He is the author/editor of 17 academic books and 21 book chapters. He serves as a member for the Editorial Board for several international journals, including *IEEE Communications Magazine* and *IET Wireless Sensor Systems*. He has received a number of prizes and scholarships, including the Best Student Prize (Loughborough University), Commonwealth Scholarship, and Overseas Research Scholarship (ORS) conferred by the Committee of Vice Chancellors and Principals (CVCP) in the U.K.

SOTIRIOS K. GOUDOS (Senior Member, IEEE) received the B.Sc. degree in physics, the M.Sc. degree in electronics, and the Ph.D. degree in physics from the Aristotle University of Thessaloniki, in 1991, 1994, and 2001, respectively, the master's degree in information systems from the University of Macedonia, Greece, in 2005, and the Diploma degree in electrical and computer engineering from the Aristotle University of Thessaloniki, in 2011. He joined the Department of Physics, Aristotle University of Thessaloniki, in 2013, where he is currently an Associate Professor. He is the Director of the ELEDIA@AUTH and a Laboratory Member of the ELEDIA Research Center Network. He is the author of the book *Emerging Evolutionary Algorithms for Antennas and Wireless Communications* (The Institution of Engineering and Technology, 2021). His research interests include antenna and microwave structures design, evolutionary algorithms, wireless communications, and semantic web technologies. He is a member of the IEICE, the Greek Physics Society, the Technical Chamber of Greece, and the Greek Computer Society. He is the founding Editor-in-Chief of the *Telecom* open access journal (MDPI). He is serving as an Associate Editor for IEEE TRANSACTIONS ON ANTENNAS AND PROPAGATION, IEEE ACCESS, and IEEE OPEN JOURNAL OF THE COMMUNICATION SOCIETY. He is serving as the IEEE Greece Section Secretary.